Int J Clin Exp Med 2015;8(4):5217-5226
www.ijcem.com /ISSN:1940-5901/IJCEM0006187

Original Article

Anatomy and CT reconstruction of the anterior area of sphenoid sinus

Shousen Wang*, Jinchao Zhang*, Liang Xue*, Liangfeng Wei, Zhiyu Xi, Rumi Wang

Department of Neurosurgery, Fuzhou General Hospital, Fujian Medical University, Fuzhou 350025, P. R. China.
**Equal contributors.*

Received January 21, 2015; Accepted March 14, 2015; Epub April 15, 2015; Published April 30, 2015

Abstract: Background: The anatomical structures of anterior area of sphenoid sinus are observed by CT reconstruction of radiographic images in some studies. However, the detailed anatomic information of the extended transsphenoidal approach is still incomplete. Method: Fifteen cases (30 sides) of adult cadaveric skulls and 20 cases (40 sides) of bleached adult dry skulls were observed and measured under microscope. CT imaging data were obtained from 12 patients. Results: Anatomy of anterior area of sphenoid sinus and sphenopalatine artery observed from CT three-dimensional reconstructed images was consistent with that observed from adult cadaveric skulls and bleached adult dry skulls. The anterior sphenoid sinus wall resembled a bird head, with midline protrude prismatically. The sphenoid ostia on both sides were in shape of bird-eyes, and the sphenoidal rostrum below was like the beak. The "shallowest point" was firstly reported in this study and was defined as the nearest point from the nostril to the anterior sphenoid sinus wall. It was located about 5.5 mm from sphenoid sinus ostium, and 5 mm from the upper edge of the posterior choanae. It was an important anatomical reference mark in locating the sphenoid sinus ostium in the anterior sinus wall. Conclusion: The three-dimensional images reconstructed by CT scan can visually display the bone structure of anterior area of sphenoid sinus, sphenopalatine artery and its main branches. Virtual endoscopy reconstruction can confirm the structural details of CT reconstruction and simulate transsphenoidal surgery.

Keywords: Transsphenoidal surgery, sphenoid sinus ostium, sphenopalatine artery, microsurgical anatomy, CT, three-dimensional reconstruction

Introduction

The trauma of transsphenoidal resection of pituitary adenoma through unilateral endonasal transsphenoidal approach is significantly reduced than that through the sublabial approach [1]. The extended endonasal approach can remove pituitary adenomas that extend forward, backward or sideways and lesions in the upper clivus [2-7]. The above surgery approaches should be guided by the anatomical landmarks of the anterior wall and the sphenoid sinus ostia. To accurately guide the approach and direction of surgery and to open the anterior sphenoid sinus wall in a safe and convenient way, it is very important to identify the anatomical features of individual patient.

It is very important to identify the morphological features and variations of nasal septum, sphenopalatine artery, sphenoid sinus ostia and structures within the sphenoid sinus on radiographic images. Routine MR and CT imaging can only provide two-dimensional anatomy images. These two-dimensional images are different from three-dimensional structures observed in the operation and in the specimens. And surgical risk can be increased if surgeries are performed based on the information from two-dimensional images. The three-dimensional CT reconstruction and virtual endoscopy reconstruction can directly reveal the anatomical structures and their adjacent structures for the surgical approach.

In some studies, the morphology of sphenoid sinus and its ostium is observed through unilateral endonasal transsphenoidal approach [8, 9]. The anatomical structures of anterior area of sphenoid sinus are observed by CT reconstruction of radiographic images [10-12]. However, the detailed anatomic information of the extended transsphenoidal approach is still incomplete. This study aims to observe and measure the anatomy of the anterior sphenoid sinus wall and its adjacent structures in dry skulls and cadaveric skulls through unilateral endonasal transsphenoidal approach. CT scans were performed in patients with spontaneous subarachnoid hemorrhage to reconstruct the radiographic images of sphenoid sinus. The transsphenoidal approach was simulated by the virtual endoscopy. Our results provide detailed anatomy data of sphenoid sinus for the transsphenoidal approach.

Materials and methods

Specimens and patients

Specimens of 20 bleached adult skulls and 15 adult cadaveric skulls were collected from South-eastern China area. The age of these cadaveric specimens was from 19 to 76 years old, with an average age of 32 years. There were 11 males and 4 females. The specimens were fixed in 10% formalin (Clinical Anatomy Center, Fuzhou General Hospital, Fuzhou, China). CT imaging data were obtained from 12 patients who had subarachnoid hemorrhage caused by rupture of intracranial aneurysm and underwent CT angiography. There were 7 males and 5 females, aging from 22 to 55 years old.

Prior written and informed consent were obtained from every patient or the patients' family. This study was approved by the ethics review board of Fujian Medical University.

Specimen observation

According to the requirements of transsphenoidal surgery, skull bone structure was observed and measured. Skull was sawed sagittally or coronally. Under the operating microscope, bony structures including nasal septum, turbinates, sphenoid sinus ostium, sphenopalatine foramen, sphenoid sinus, posterior ethmoid sinus, and optic canal were observed from different angles. And the corresponding anatomical features were measured. Briefly, a compass was put into nasal cavity under operating microscope to locate the corresponding structures. Then the distance between the corresponding structures was determined by measuring the distances between the two tips of compass with a vernier caliper. To determine the viewing angle, a line was drawn along the middle of the sagittal plane by a ruler. Then, the viewing angle was measured by a protractor. The midpoint of nasal columella was located at the midpoint of the midline in the front of nasal columella. The line from the midpoint of nasal columella to the lower edge of the sphenoid sinus ostia was used as the viewing angle. The sphenopalatine artery, lateral nasal artery, posterior nasal septum artery and descending palatine artery were exposed after removing the posterior wall of maxillary sinus and separating the wing palate part of maxillary artery. Their distribution and adjacent structures were observed. Surgical approach was simulated to measure the location of sphenoid sinus ostium and its relations with sphenopalatine foramen. A straight probe was stretched from the nostril to the anterior sphenoid sinus wall, to determine the nearest point on the anterior sphenoid sinus wall, which was defined as the "shallowest point". Then the "shallowest point" was recorded and measured as above described.

Clinical CT

GE Discovery Ultra 16-slice spiral CT scanner (New Jersey, USA) was used for CT scan. The parameters included 0.5 s rotation time, 0.625 mm or 1.25 mm thickness, 0.625 mm space, 0.275:1 pitch, 1.2 s imager scan distance, 250 mm field of view, 512 × 512 matrix, 140 Kv tube voltage and 180 mAs tube current. Patients were in supine position, and received intravenous injection of contrast medium Omnipaque through the cubital vein using high-pressure syringe. The dose of Omnipaque was 2 ml/kg and the flow rate was 2.5 to 3.5 ml/s. When CT value of target vessel reached the preset threshold, Smart Prep scanning system was started to complete the scanning process. After scanning, original data of CT scan were first used for cross-sectional reconstruction, and then further analyzed by the ADW4.1 Advanced Workstation. The cross-sectional images were used for volume rendering (VR), multiplanar reformation (MPR) and virtual endoscopy (VE), respectively. Finally, the three-dimensional and virtual endoscopy images of nasal septum, anterior area of sphenoid sinus, sphenopalatine foramen, sphenopalatine artery, and sphenoid sinus were constructed.

Statistical analysis

Measurement data of each group was expressed as mean ± standard deviation (SD), using SPSS13.0 statistical software.

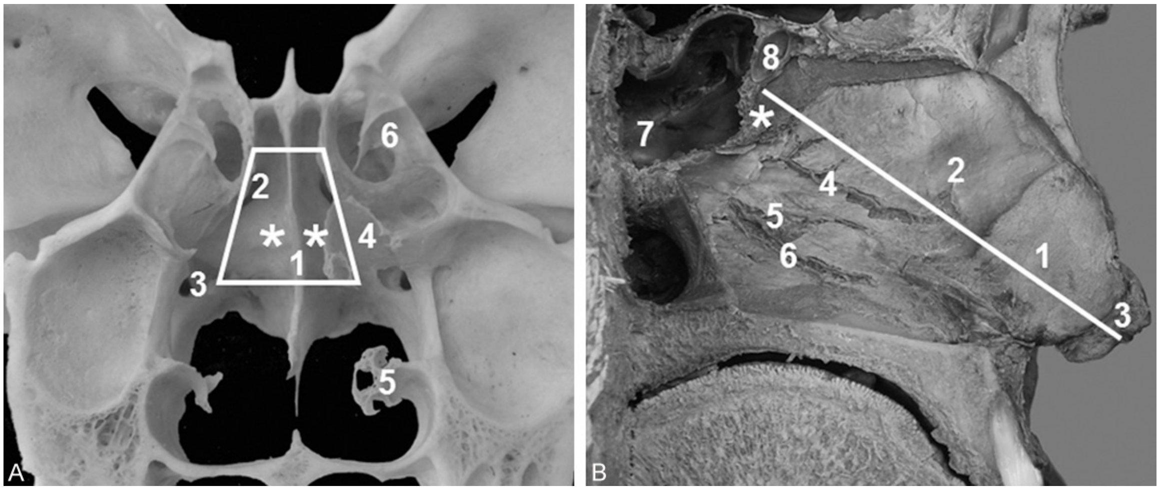

Figure 1. Autopsy observation of anterior area of sphenoid sinus. A: Skull specimens were sawn along the coronal way, and anterior area of sphenoid sinus was observed from the front to show its range and anatomy. Numbers in this figure indicated the following structures: 1. Nasal septum; 2. Sphenoid ostium; 3. Sphenopalatine foramen; 4. Middle turbinate; 5. Lower turbinate; 6. Posterior ethmoid cell. The trapezoidal area in the figure indicated the traditional surgical opening of anterior area of sphenoid sinus. The white symbol "*" indicated the location of the "shallowest point". B: Preservative cadaveric head specimens were sawn along the median sagittal way and dissected through nasal mucosal to reveal posterior nasal septum artery. The nasal septum of the right side was shown. Numbers in this figure indicated the following structures: 1. Septal nasal cartilage; 2. Perpendicular plate of ethmoidal bone; 3. Lateral nasal cartilage; 4. Upper branch of posterior septum artery; 5. Lower branch of posterior septum artery; 6. Sphenopalatine nerve; 7. Sphenoid sinus; 8. Ethmoid sinus cell. The white line indicated the nasal surgical path. The white symbol "*" indicated the location of the "shallowest point".

Results

Anatomy of anterior area of sphenoid sinus

The anatomical features of anterior area of sphenoid sinus, including sphenoid sinus ostium, sphenopalatine foramen and the "shallowest point", were shown in **Figure 1**. The surgical opening of the anterior sphenoid sinus wall was indicated in **Figure 1A** as the trapezoidal area, which was enclosed by sphenoid sinus ostia of both sides and sphenopalatine foramen. Among the 70 sides of specimens, there were 36 sides (51%) with sphenoid sinus ostium in round shape, 20 sides (29%) in oval shape, and 14 sides (20%) in ovoid shape. The measurement data of sphenoid sinus ostia of both sides were shown in **Table 1**. The large diameter (length) of sphenoid sinus ostium on the left side was 5.6 ± 0.3 mm (4.9 mm to 5.9 mm), and the short diameter (width) on the left side was 3.6 ± 0.2 mm (3.1 mm to 4.0 mm). The sphenoid sinus ostium was 12.2 ± 1.0 mm from the posterior choanae. Sphenopalatine foramen was located below and lateral to the sphenoid sinus ostium and at the rear of middle turbinate, with distance of 6.9 ± 1.4 mm to sphenoid sinus ostium. The distance from upper edge of sphenoid sinus ostium to cribriform plate was 11.6 ± 3.1 (9.4 to 12.8) mm.

The anatomy and location of sphenopalatine foramen was also shown in **Figure 1A**. Among the 70 sides of specimens, there were 10 sides of sphenopalatine foramen with round shape, 37 sides with oval shape, 5 sides with triangular shape, and 18 sides with irregular shape. There were 61 sides with only one sphenopalatine foramen, and some of them had a secondary foramen. There were 8 sides with two foramens, and 1 side with three foramens. The height of sphenopalatine foramen was 6.09 ± 0.69 mm (4.28 mm to 7.47 mm) and the width of sphenopalatine foramen was 5.24 ± 0.57 mm (4.12 mm to 6.19 mm). The distance between the medial edges of sphenopalatine foramen on both sides was 18.23 ± 2.46 mm.

The "shallowest point" was the nearest point from nostril to the anterior sphenoid sinus wall, locating at about 5 mm above the upper edge of the posterior choanae and at the joint between vomer and sphenoid (**Figure 1A** and **1B**). This "shallowest point" was also located inferior and medial to sphenoid sinus ostia, and

Table 1. Measurement data of sphenoid sinus ostium

Distance (mm)	Left side (n = 35)	Right side (n = 35)
Length	5.6 ± 0.3 (4.9~5.9)	5.67 ± 0.4 (5.0~5.7)
Width	3.6 ± 0.2 (3.1~4.0)	3.5 ± 0.2 (3.3~3.9)
Sinus ostium-the posterior choanae	12.0 ± 1.1 (9.5~13.8)	12.4 ± 0.8 (9.9~12.7)
Sinus ostium-rear part of upper turbinate	9.8 ± 0.8 (9.1~11.5)	9.2 ± 0.9 (8.5~12.1)
Sinus ostium-rear part of middle turbinate	19.5 ± 1.1 (16.9~21.1)	19.5 ± 1.4(16.5~20.4)
Sinus ostium- Sphenopalatine foramen	6.9 ± 1.2 (4.6~8.9)	6.9 ± 1.6 (4.9~10.0)

Note: Data were expressed as mean ± SD. The minimum value and the maximum value were given in brackets.

Table 2. Measurement data of the shallowest point

Distance (mm)	Left side (n = 15)	Right side (n = 15)
The shallowest point-columella nasi	64.1 ± 4.9 (55.5~74.1)	64.5 ± 5.1 (56.5~73.8)
The shallowest point-lower edge of sphenoid sinus ostium	5.2 ± 0.4 (3.9~7.4)	5.8 ± 0.4 (4.2~7.1)
The shallowest point-middle point of sphenoid sinus ostium	7.0 ± 0.4 (6.4~8.2)	7.4 ± 0.4 (6.9~8.9)
The shallowest point-the posterior choanae	5.2 ± 0.3 (4.9~7.2)	5.0 ± 0.3 (4.5~6.8)
The shallowest point-anterior nasal spine	54.3 ± 4.4 (47.8~58.1)	54.7 ± 4.7 (51.5~59.9)

Note: Data were expressed as mean ± SD. The minimum value and the maximum value were given in brackets.

above and medial to the sphenopalatine foramen. From the sagittal plane, the "shallowest point" was located at the leading edge of the anterior sphenoid sinus wall. The measurement results of the "shallowest point" were shown in **Table 2**.

Anatomy of sphenopalatine artery

The anatomical features of sphenopalatine artery and its main branches in 30 sides of cadaveric skull specimens were shown in **Figure 2A** and **2B**. There were 17 sides (56.7%) of sphenopalatine artery branching before exiting sphenopalatine foramen, and 13 sides (43.3%) branching after exiting sphenopalatine foramen. The outer diameters of sphenopalatine artery, lateral nasal artery and posterior nasal septal artery were 2.1 ± 0.5 mm (1.5 mm to 2.4 mm), 1.8 ± 0.4 mm (1.5 mm to 2.0 mm) and 1.7 mm ± 0.4 mm (1.4 mm to 2.1 mm), respectively. The distance from sphenoid sinus ostium to upper branch of nasal septum artery was 8.2 ± 0.5 (6.6 to 12.2) mm.

According to the branching site of sphenopalatine artery, the branching pattern can be classified as four types of Type I, Type II, Type III and Type IV (**Figure 2C**). In Type I, the sphenopalatine artery divided into lateral nasal artery and posterior nasal septum artery after exiting sphenopalatine foramen. In type II, sphenopalatine artery divided into two branches before entering sphenopalatine foramen and these two branches entered the nasal cavity through sphenopalatine foramen together. In type III, the artery was divided into two branches before sphenopalatine foramen, and entered the nasal cavity through sphenopalatine main foramen and secondary foramen, respectively. Type IV was similar to type III. However, the posterior nasal septum artery divided into two branches before exiting the sphenopalatine foramen and the two branches passed through main foramen simultaneously. There were 5 sides with type I (16.7%), 7 sides with type II (23.3%), 8 sides with type III (26.7%) and 10 sides with type IV (33.3%).

The posterior nasal septum artery is the end branch of sphenopalatine artery. The posterior nasal septum artery can be classified as three types of Type I, Type II and Type III (**Figure 2D**). In type I, the stem of posterior nasal septum artery exited the sphenopalatine foramen and branched outside the sphenopalatine foramen. A total of 5 sides (16.7%) had type I. In type II, the posterior nasal septum artery itself entered the sphenopalatine foramen and branched after exiting the sphenopalatine foramen. There were 15 sides with type II (50%). In type III, the posterior nasal septum artery branched before

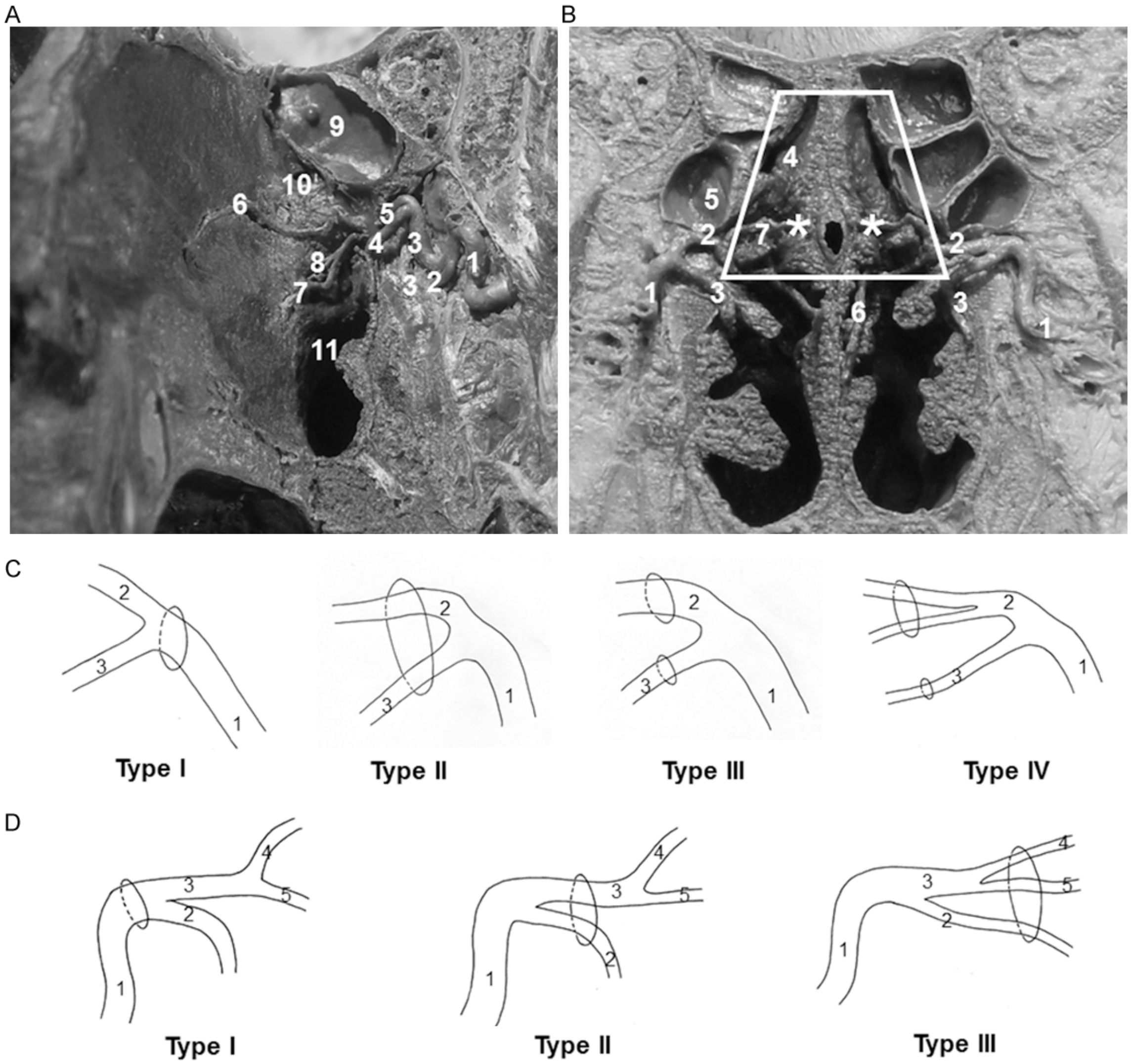

Figure 2. Anatomy of sphenopalatine artery and its branches. A: The anterior part of preservative cadaveric head specimen was sawn along the median sagittal way, and along the coronal way at the level of the sphenopalatine foramen, to reveal sphenopalatine artery and its branches. The view observed from the left front way was shown. Numbers in this figure indicated the following structures: 1. Maxillary artery; 2. Sphenoid descending artery; 3. Sphenopalatine artery; 4. Lateral nasal artery; 5. Posterior nasal septum artery; 6. Upper branch of posterior septum artery; 7. Lower branch of posterior septum artery; 8. Sphenopalatine nerve; 9. Posterior ethmoid cell; 10. Sphenoid ostium; 11. The posterior choanae. B: The preservative cadaveric head specimen was sawn along the coronal way at the level of sphenopalatine foramen, to reveal sphenopalatine artery and its branches of both sides. Numbers in this figure indicated the following structures: 1. Sphenopalatine artery; 2. Posterior nasal septum artery; 3. Lateral nasal artery; 4. Sphenoid ostium; 5. Posterior ethmoid cell; 6. Lower branch of posterior nasal septum artery; 7. Upper branch of posterior nasal septum artery. The white symbols of "*" indicated the location of the "shallowest point". C: Schematics of branches of left sphenopalatine artery (front view), including branching Type I, Type II, Type III and Type IV. Numbers in this figure indicated the following structures: 1. Sphenopalatine artery; 2. Posterior nasal septum artery; 3. Lateral nasal artery. The oval indicated sphenopalatine foramen, and the small oval indicated the secondary sphenopalatine foramen. D: Schematics of branches of right sphenopalatine artery (front view), including branching Type I, Type II and Type III. Numbers in this figure indicated the following structures: 1. Sphenopalatine artery; 2. Lateral nasal artery; 3. Posterior nasal septum artery; 4. Upper branch of posterior nasal septum artery; 5. Lower branch of posterior nasal septum artery. Oval indicated sphenopalatine foramen.

entering sphenopalatine foramen. There were 10 sides with type III (33.3%). There were 21 sides (70%) of two branches, 3 cases (23.3%) of three branches, and 2 cases (6.7%) more than 3 branches.

CT image analysis and three-dimensional reconstruction

CT images were collected from 12 patients. The three-dimensional reconstructed CT image

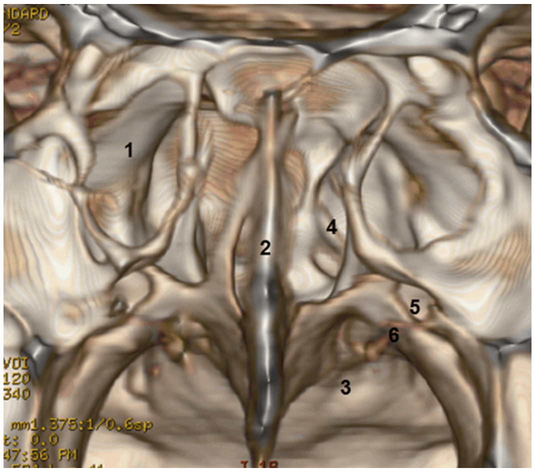

Figure 3. CT three-dimensional reconstruction of anterior area of sphenoid sinus. CT images were collected from 12 patients. The front view of anterior area of sphenoid sinus was shown. The sphenoid ostium and sphenopalatine foramen were close to each other. Posterior nasal septum artery passed through lower edge of sphenopalatine foramen, then divided into two branches and extended to nasal septum along the anterior sphenoid sinus wall. Numbers in this figure indicated the following structures: 1. Posterior ethmoid cell; 2. Nasal septum; 3. The posterior choanae; 4. Sphenoid ostium; 5. Sphenopalatine foramen; 6. Posterior septum artery.

of anterior area of sphenoid sinus was shown in **Figure 3**. Sphenoid sinus ostium was located at the rear of upper turbinate. There were 8 cases of bilateral sphenoid sinus ostia on the same scanning planes, and 4 cases on different scanning planes. There were 24 sides with identifiable bone sphenoid sinus ostia, and 5 sides with unidentifiable mucosa sphenoid sinus ostia. The long diameter of sphenoid sinus ostium was (5.81 ± 0.36) mm, and short diameter was (3.64 ± 0.24) mm. The maximum distance between two sphenoid sinus ostia was (14.34 ± 2.32) mm. Structures including sphenoid sinus ostia, the anterior sphenoid sinus wall, top part of nasal cavity, upper nasal turbinate, sphenopalatine foramen, sphenoid sinus and its septations were shown in the reconstructed images (**Figure 3**). There were 14 sides of sphenoid sinus ostia in round shape, and 10 sides in oval shape. These results suggest that the three-dimensional CT image of sphenoid sinus and ethmoid sinus was successfully reconstructed.

There were 10 sides of sphenopalatine foramen in round shape, 10 sides in oval shape, and 4 sides in irregular shape. There were 22 sides with one foramen and 2 sides with two foramens. The long diameter was (6.24 ± 0.71) mm, and short diameter was (5.31 ± 0.53) mm. The distance between the medial edges of both foramens was (18.63 ± 2.12) mm. There were four types of sphenopalatine arteries in the coronal plane (**Figure 4**), including M type of sphenopalatine artery (**Figure 4A**), Intermediate type of sphenopalatine artery (**Figure 4B**), Y type of sphenopalatine artery (**Figure 4C**) and T type sphenopalatine artery (**Figure 4D**). The upper part of **Figure 4** showed the different types of sphenopalatine artery on CT three-dimensional reconstruction images. The lower part of **Figure 4** showed the schematics of the different types of sphenopalatine artery. However, this CT angiography method was not effective in showing small arteries. The reveal rates of different segment of sphenopalatine artery were shown in **Table 3**.

Transsphenoidal surgery was simulated to reconstruct the anterior area of sphenoid sinus (**Figure 5**). Virtual endoscopy was introduced into the sphenoid sinus through the unilateral nostril and the sphenoid sinus ostium. The sellar protuberance protruded into the sphenoid sinus from the back-up side of the sphenoid sinus. **Figure 5A** showed the dynamic image under virtual endoscopy. The corresponding structures on CT images were shown in **Figure 5B** (axial CT image), **Figure 5C** (coronal CT image), and **Figure 5D** (sagittal CT image).

Discussion

In this study, we proposed the concept of the "shallowest point" when performing transsphenoidal surgery. The "shallowest point" was defined as the nearest point from the nostril to the anterior sphenoid sinus wall. During simulated transsphenoidal surgery on cadaveric skulls, the "shallowest point" was found beneath the sphenoid sinus ostia and above and medial to sphenopalatine foramen. It was located about 5.5 mm from sphenoid sinus ostium, and 5 mm from the upper edge of the posterior choanae. We suppose that the "shallowest point" is an important anatomical reference mark in locating the sphenoid sinus ostium in the anterior sinus wall. The "shallowest point" has not been reported previously. Anatomy features of sphenopalatine foramen and sphenopalatine artery branches of cadaveric skulls were observed and analyzed. The distance from sphenopalatine foramen to

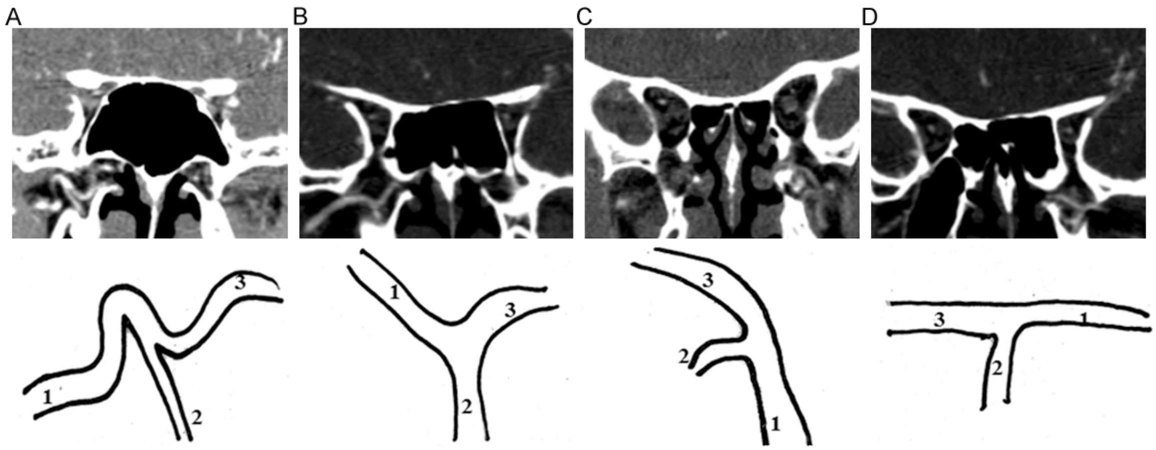

Figure 4. Sphenopalatine artery on CT three-dimensional reconstruction images (coronal view). CT images were collected from 12 patients. The upper part showed the different types of sphenopalatine artery on CT three-dimensional reconstruction images. The lower part showed the schematics of the different types of sphenopalatine artery. A: M type of sphenopalatine artery. B: Intermediate type of sphenopalatine artery. C: Y type of sphenopalatine artery. D: T type sphenopalatine artery. Numbers in this figure indicated the following structures: 1. Maxillary artery; 2. Descending palatine artery; 3. Sphenopalatine artery.

Table 3. Reveal rate of different segment of sphenopalatine artery in three-dimensional reconstructed CT image

	Artery reveal rate	Artifacts and nonreveal rate
Trunk of sphenopalatine artery	100% (24/24)	0% (0/24)
Lateral nasal artery	91.7% (22/24)	8.3% (2/24)
Posterior nasal septum artery	87.5% (21/24)	12.5% (3/24)
Upper branch of posterior nasal septum artery	75% (18/24)	25% (6/24)
Lower branch of posterior nasal septum artery	70.8% (17/24)	29.3% (7/24)
Total	87.5% (126/144)	12.5% (18/144)

sphenoid sinus ostium was about 7 mm. The above mentioned information was important to identify structures of sphenopalatine foramen and sphenopalatine artery, and to stop bleeding during transsphenoidal surgery. Furthermore, these results from cadaveric skulls were confirmed by data from CT reconstructed images.

Unilateral endonasal transsphenoidal approach may cause intraoperative bleeding in the anterior area of sphenoid sinus, which is usually due to bleeding of posterior nasal septum artery or sphenopalatine artery [13-20]. Sphenopalatine foramen is located below and lateral to the sphenoid sinus ostium, with distance of about 7 mm from sphenoid sinus ostium and about 9 mm from midline. And, the distance from sphenoid sinus ostium to the upper branch of septum artery is about 8 mm. The above three distance data are important reference markers to identify sphenopalatine foramen and to avoid injuries to main arteries during transsphenoidal surgery. After transsphenoidal surgery, tardive nasal bleeding could occur from time to time. Tardive nasal bleeding is often associated with injuries of the sphenopalatine artery and septum artery, with occurrence rate of about 0.5% to 2% [13-15]. Raymond et al analyzed arterial injuries in 1800 cases of transsphenoidal surgeries. They found that there were 21 cases of nasal bleeding, 17 cases of internal carotid artery injury, 4 cases of sphenopalatine artery injury, and 4 deaths [13]. Cavallo et al reported 3 cases of sphenopalatine artery bleeding and 1 case of septum artery bleeding in 250 cases of transsphenoidal surgeries [14]. In another study by Cappabianca et al, there were 2 cases of sphenopalatine artery bleeding in 146 cases of transsphenoidal surgeries. Bleeding occurred at 2 to 30 days after surgery, with total amount of bleeding up to 1000 ml. And, there was also repeated bleeding [15].

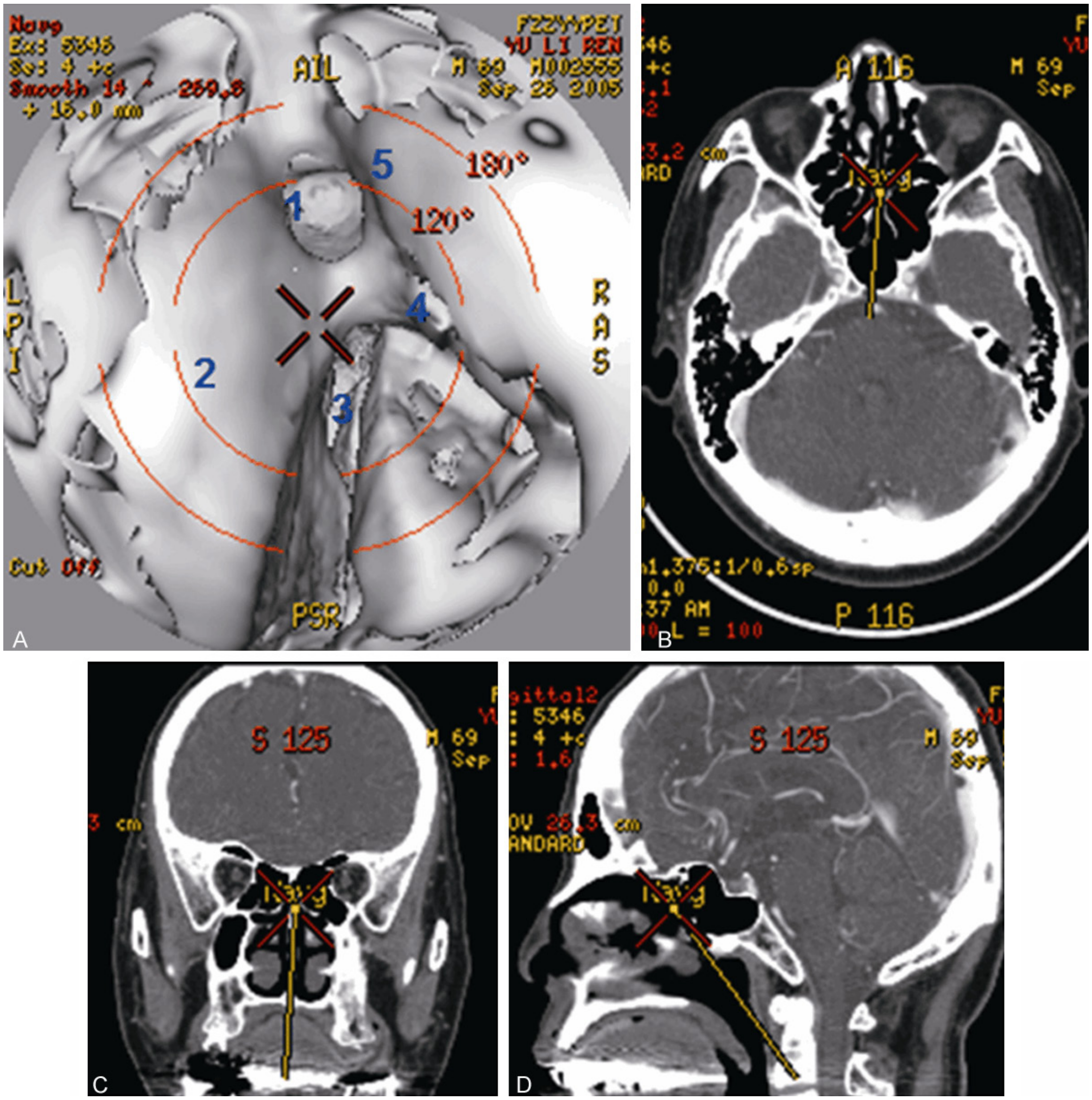

Figure 5. Simulated transsphenoidal surgery by virtual endoscopy. This figure showed three-dimensional anatomy image and corresponding structure on routine CT. A: Reconstruction image by virtual endoscopy. Numbers in this figure indicated the following structures: 1. Sphenoid sinus ostium; 2. Nasal septum; 3. The posterior choanae; 4. Sphenopalatine foramen; 5. Upper turbinate. "×" indicated the position of endoscopic lens. B-D: Corresponding axial, coronal and sagittal CT images were shown. "×" indicated the position of endoscopic lens and the yellow line indicated the moving path of endoscopy.

Based on CT images, three-dimensional model of nasal anatomy structures can be established without distortion and with high resolution. With this three-dimensional model, nasal anatomy structures can be observed from different angles and adjacent relations between structures can be displayed [21]. In this experiment, CT could identify whether the bone sphenoid sinus ostia of both sides were on the same plane, determine the heights of sphenoid sinus ostia and discriminate them accurately during surgery. Reconstructed image can be observed three-dimensionally, virtually and dynamically and can be revised to better reveal the nasal anatomy structures. It can also avoid surgical damages on patients, and help surgical planning and clinical teaching.

The anterior sphenoid sinus wall resembled a bird head, with midline protrude prismatically. The sphenoid ostia on both sides were in shape of bird-eyes, and the sphenoidal rostrum below was like the beak. The characteristics of these structures are important anatomical landmarks during surgery. The sphenoid sinus ostium was located in the anterior sphenoid sinus wall, with distance of about 12 mm from upper edge of the posterior choanae. The difference in the location of sphenoid sinus ostium may be due to ethnic differences. We first reported the "shallowest point" in the anterior sphenoid sinus wall. It was located between the lower edge of sphenoid sinus ostium and the upper edge of posterior choanae. Posterior nasal septum artery passed under the "shallowest point". Sphenopalatine foramen was located at 7 mm below and lateral to sphenoid sinus ostium. This information could be used to identify sphenopalatine foramen and sphenopalatine artery during surgery. CT three-dimensional reconstruction of the anterior sphenoid sinus wall could be used in preoperative anatomical assessment of unilateral endonasal transsphenoidal surgery. Reconstruction of CT virtual endoscopy can provide dynamic and three-dimensional anatomical details of the anterior sphenoid sinus wall, thus reducing surgical risk. However, the virtual endoscopy has some disadvantages that limit its application. For example, under virtual endoscopy, the normal color of mucosa and bone cannot be displayed. And, the images lack the sense of texture. Additionally, the virtual endoscopy can only provide the space location of anatomical structures. Unlike the real endoscopy, the virtual endoscopy cannot directly go through the narrow channel of the mucosa ostium. Thus, prospective/pilot studies are still needed to objectively assess the benefit of such techniques.

Acknowledgements

We want to thank Heping Zheng, Associate Professor from Clinical Anatomy Center of Fuzhou General Hospital, for the preparation of anatomical specimens.

Disclosure of conflict of interest

None.

Address correspondence to: Dr. Shousen Wang, Department of Neurosurgery, Fuzhou General Hospital, Fujian Medical University, No. 156 Xihuanbei Road, Fuzhou 350025, P. R. China. Tel: 86-591-24937080; Fax: 86-591-87640785; E-mail: wangss1965@126.com

References

[1] Griffith HB and Veerapen R. A direct transnasal approach to the sphenoid sinus. Technical note. J Neurosurg 1987; 66: 140-142.

[2] Jho H and Jho D. Use of endoscopic techniques for pituitary adenoma resection. Endocrinologist 2004; 14: 76-86.

[3] Couldwell WT. Transsphenoidal and transcranial surgery for pituitary adenomas. J Neurooncol 2004; 69: 237-256.

[4] Shou X, Li S, Wang Y, Zhao Y, Jia P and Zhou L. Treatment of pituitary adenomas with a transsphenoidal approach. Neurosurgery 2005; 56: 249-256; discussion 249-256.

[5] Wang Q, Lan Q and Lu X. Extended endoscopic endonasal transsphenoidal approach to the suprasellar region: anatomic study and clinical considerations. J Clin Neurosci 2010; 17: 342-346.

[6] Laws ER, Kanter AS, Jane JA and Dumont AS. Extended transsphenoidal approach. J Neurosurg 2005; 102: 825-827; discussion 827-828.

[7] Abuzayed B, Tanriover N, Akar Z, Eraslan BS and Gazioglu N. Extended endoscopic endonasal approach to the suprasellar parachiasmatic cisterns: anatomic study. Childs Nerv Syst 2010; 26: 1161-1170.

[8] Campero A, Emmerich J, Socolovsky M, Martins C, Yasuda A, Agustín Campero A and Rhoton A. Microsurgical anatomy of the sphenoid ostia. J Clin Neurosci 2010; 17: 1298-1300.

[9] Lazaridis N, Natsis K, Koebke J and Themelis C. Nasal, sellar and sphenoid sinus measurements in relation to pituitary surgery. Clin Anat 2010; 23: 629-636.

[10] Hwang SH, Joo YH, Seo JH, Cho JH and Kang JM. Analysis of sphenoid sinus in the operative plane of endoscopic transsphenoidal surgery using computed tomography. Eur Arch Otorhinolaryngol 2014; 271: 2219-2225.

[11] Göçmez C, Göya C, Hamidi C, Teke M, Hattapoğlu S and Kamaşak K. Evaluation of the surgical anatomy of sphenoid ostium with 3D computed tomography. Surg Radiol Anat 2014; 36: 783-788.

[12] Kasemsiri P, Solares CA, Carrau RL, Prosser JD, Prevedello DM, Otto BA, Old M and Kassam AB. Endoscopic endonasal transpterygoid approaches: anatomical landmarks for planning the surgical corridor. Laryngoscope 2013; 123: 811-815.

[13] Raymond J, Hardy J, Czepko R and Roy D. Arterial injuries in transsphenoidal surgery for pituitary adenoma; the role of angiography and endovascular treatment. AJNR Am J Neuroradiol 1997; 18: 655-665.

[14] Cavallo LM, Briganti F, Cappabianca P, Maiuri F, Valente V, Tortora F, Volpe A, Messina A, Elefante A and De Divitiis E. Hemorrhagic vascular complications of endoscopic transsphenoidal surgery. Minim Invasive Neurosurg 2004; 47: 145-150.

[15] Cappabianca P, Cavallo LM, Colao A and de Divitiis E. Surgical complications associated with the endoscopic endonasal transsphenoidal approach for pituitary adenomas. J Neurosurg 2002; 97: 293-298.

[16] Antunes Scanavini AB, Navarro JAC, Megale SR, Lima RS and Anselmo-Lima WT. Morphometric evaluation of the sphenopalatine foramen for endonasal surgery. Rhinology 2010; 48: 441-445.

[17] Eladl HM, Khafagy YW and Abu-Samra M. Endoscopic cauterization of the sphenopalatine artery in pediatric intractable posterior epistaxis. Int J Pediatr Otorhinolaryngol 2011; 75: 1545-1548.

[18] Gupta T, Aggarwal A and Sahni D. Anatomical landmarks for locating the sphenoid ostium during endoscopic endonasal approach: a cadaveric study. Surg Radiol Anat 2013; 35: 137-142.

[19] Shires CB, Boughter JD and Sebelik ME. Sphenopalatine artery ligation: a cadaver anatomic study. Otolaryngol Head Neck Surg 2011; 145: 494-497.

[20] Prades JM, Asanau A, Timoshenko AP, Faye MB and Martin C. Surgical anatomy of the sphenopalatine foramen and its arterial content. Surg Radiol Anat 2008; 30: 583-587.

[21] Wang SS, Xue L, Jing JJ and Wang RM. Virtual reality surgical anatomy of the sphenoid sinus and adjacent structures by the transnasal approach. J Craniomaxillofac Surg 2012; 40: 494-499.